

promoting access to White Rose research papers



Universities of Leeds, Sheffield and York
<http://eprints.whiterose.ac.uk/>

This is the published version of an article in **Langmuir**

White Rose Research Online URL for this paper:

<http://eprints.whiterose.ac.uk/id/eprint/75844>

Published article:

Zhou, DJ, Ying, LM, Hong, X, Hall, EA, Abell, C and Klenerman, D (2008) *A Compact Functional Quantum Dot-DNA Conjugate: Preparation, Hybridization and Specific Label-free DNA Detection*. *Langmuir*, 24 (5). 1659 - 1664. ISSN 0743-7463

<http://dx.doi.org/10.1021/la703583u>

A Compact Functional Quantum Dot–DNA Conjugate: Preparation, Hybridization, and Specific Label-Free DNA Detection

Dejian Zhou,^{†,||} Liming Ying,[‡] Xin Hong,[§] Elizabeth A. Hall,[§] Chris Abell,[†] and David Klenerman^{*,†}

Department of Chemistry, University of Cambridge, Lensfield Road, Cambridge CB2 1EW, United Kingdom, Molecular Medicine, National Heart and Lung Institute, Imperial College London, London SW7 2AZ, United Kingdom, and Institute of Biotechnology, University of Cambridge, Tennis Court Road, Cambridge CB2 1QT, United Kingdom

Received November 16, 2007. In Final Form: January 2, 2008

In this letter, we report the preparation of a compact, functional quantum dot (QD)–DNA conjugate, where the capturing target DNA is directly and covalently coupled to the QD surface. This enables control of the separation distance between the QD donor and dye acceptor to within the range of the Förster radius. Moreover, a tri(ethylene glycol) linker is introduced to the QD surface coating to effectively eliminate the strong, nonspecific adsorption of DNA on the QD surface. As a result, this QD–DNA conjugate hybridizes specifically to its complementary DNA with a hybridization rate constant comparable to that of free DNAs in solution. We show this system is capable of specific detection of nanomolar unlabeled complementary DNA at low DNA probe/QD copy numbers via a “signal-on” fluorescence resonance energy transfer (FRET) response.

Introduction

The unique size-dependent, narrow, symmetric, bright, and stable fluorescence of quantum dots (QDs) have made them powerful tools for studying a wide range of biological problems, from biological imaging and cell tracking and trafficking to novel multiplexed sensors.¹ The broad absorption and narrow emission spectra of the QDs make them excellent donors in fluorescence resonance energy transfer (FRET)-based sensors, because these fluorescence characteristics allow the selection of a wide range of excitation wavelengths to reduce dye (acceptor) direct excitation, and proper narrow bandpass filters for the effective separation of the donor and acceptor fluorescence.^{2–4} To date, many of the QD FRET-based sensors have used protein–QD

conjugates, for example, the maltose binding protein (MBP)–QD³ or the streptavidin–QD⁴ systems. The capturing biomolecule is often linked to the QD (mostly CdSe/ZnS core/shell-based) via a relatively large linker protein, that is, streptavidin.⁴ The overall size of the QD donor is made up of the QD core/shell nanocrystal, and the surface capping and bioconjugation. The radius of the core/shell nanocrystal determines the color of fluorescence emission, which varies from ~1 nm for a 520 nm QD to 2.6 nm for a 620 nm QD.⁵ The thickness of the surface capping and bioconjugation can vary significantly, from 0.5 to 15 nm, depending on the capping methods. A typical Förster distance R_0 , a distance that produces 50% FRET efficiency, for the QD (donor)–dye (acceptor) FRET systems is between 4–7 nm.^{2–4} Since the FRET efficiency strongly depends on the donor–acceptor distance, it is important to develop a compact QD–biomolecule conjugate to reduce the FRET distance.

Currently, most water-soluble QDs are based on either wrapping with an amphiphilic polymer or encapsulating within a lipid micelle. These produce highly stable water-soluble QDs. However, these QDs are relatively large, with a hydrodynamic radius typically > 10 nm, greater than the R_0 for most QD–dye FRET systems, even before bioconjugation.⁵ The relatively large size of the water-soluble QD and the linker protein is a limiting factor that often leads to low FRET efficiencies, especially at low target/QD copy numbers. Consequently, a high copy number of the target to each QD (usually > 10) is required to achieve high FRET efficiency.⁴ For example, at a 1:1 target DNA/QD ratio, Hohng and Ha found that the FRET efficiency between a streptavidin-coated 585 nm QD and Cy5-labeled DNA acceptor is very low, with most species being < 5.5%.^{4c} However, Wang and coauthors showed that highly efficient FRET (~90%) can be achieved by increasing the copy number of the DNA probe per QD to 54 using a streptavidin-coated 605 nm QD and Cy5-labeled DNA.^{4a} To make highly sensitive QD FRET-based sensors suitable for low target/QD copy numbers (i.e., 1:1), it is important to reduce the size of the QD donor. This can be achieved by reducing the thickness of the QD surface coating, because this

* To whom correspondence should be addressed. Telephone: +44-1223-336491. Fax: +44-1223-336 362. E-mail: dk10012@cam.ac.uk.

[†] Department of Chemistry, University of Cambridge.

[‡] Imperial College London.

[§] Institute of Biotechnology, University of Cambridge.

^{||} Current address: School of Chemistry and Astbury Centre for Structural Molecular Biology, University of Leeds, Leeds LS2 9JT, United Kingdom. E-mail: d.zhou@leeds.ac.uk.

(1) (a) Alivisatos, P. *Nat. Biotechnol.* **2004**, *22*, 47. (b) Michalet, X.; Pinaud, F. F.; Bentolila, L. A.; Tsay, J. M.; Doose, S.; Li, J. J.; Sundaresan, G.; Wu, A. W.; Gambhir, S. S.; Weiss, S. *Science* **2005**, *307*, 538. (c) Han, M.-Y.; Gao, X.; Su, J. Z.; Nie, S. *Nat. Biotechnol.* **2001**, *19*, 631. (d) Chan, W. C. W.; Nie, S. *Science* **1998**, *281*, 2016. (e) Klostranec, J. M.; Chan, W. C. W. *Adv. Mater.* **2006**, *18*, 1953.

(2) (a) Clapp, A. R.; Medintz, I. L.; Mattoussi, H. *ChemPhysChem* **2006**, *7*, 47. (b) Clapp, A. R.; Medintz, I. L.; Mauro, J. M.; Fisher, B. R.; Bawendi, M. G.; Mattoussi, H. *J. Am. Chem. Soc.* **2004**, *126*, 301. (c) Shi, L.; Paoli, V. D.; Rosenzweig, N.; Rosenzweig, Z. *J. Am. Chem. Soc.* **2006**, *128*, 10378. (d) Bakalova, B.; Zhelev, Z.; Ohba, H.; Baba, Y. *J. Am. Chem. Soc.* **2005**, *127*, 11328. (e) Ruedas-Rama, M. J.; Wang, X.; Hall, E. A. H. *Chem. Commun.* **2007**, 1544. (f) Potapova, I.; Mruk, R.; Hübner, C.; Zentel, R.; Basché, T.; Mews, A. *Angew. Chem., Int. Ed.* **2005**, *44*, 2437. (g) Gueroui, Z.; Libchaber, A. *Phys. Rev. Lett.* **2004**, *93*, 166108. (h) Lee, S. F.; Osborne, M. J. *J. Am. Chem. Soc.* **2007**, *129*, 8936. (i) Medintz, I. L.; Berti, L.; Pons, T.; Grimes, A. F.; English, D. S.; Alessandrini, A.; Facci, P.; Mattoussi, H. *Nano Lett.* **2007**, *7*, 1741.

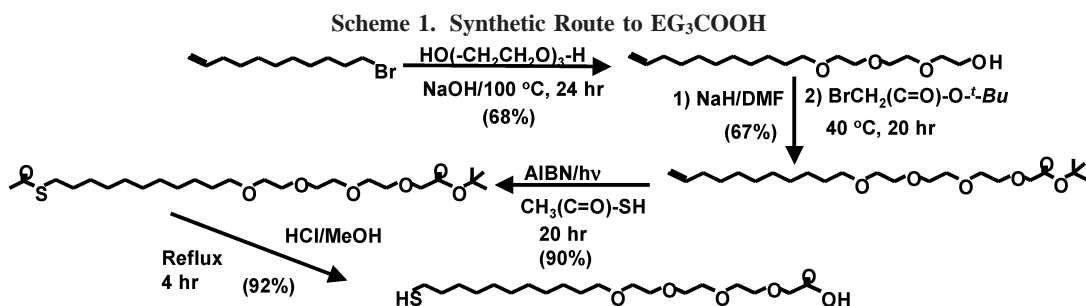
(3) (a) Medintz, I. L.; Clapp, A. R.; Mattoussi, H.; Goldman, E. R.; Fisher, B.; Mauro, J. M. *Nat. Mater.* **2003**, *2*, 630. (b) Medintz, I. L.; Konner, J. H.; Clapp, A. R.; Stanish, I.; Twigg, M. E.; Mattoussi, H.; Mauro, J. M.; Deschamps, J. R. *Proc. Natl. Acad. Sci. U.S.A.* **2004**, *101*, 9612. (c) Pons, T.; Medintz, I. L.; Wang, X.; English, D. S.; Mattoussi, H. *J. Am. Chem. Soc.* **2006**, *128*, 15324.

(4) (a) Zhang, C. Y.; Yeh, H. C.; Kuroki, M. T.; Wang, T. H. *Nat. Mater.* **2005**, *4*, 826. (b) Oh, E.; Hong, M. Y.; Lee, D.; Nam, S. H.; Yoon, H. C.; Kim, H. S. *J. Am. Chem. Soc.* **2005**, *127*, 3270. (c) Hohng, S.; Ha, T. *ChemPhysChem* **2005**, *6*, 956. (d) Levy, M.; Cater, S. F.; Ellington, A. D. *ChemBioChem* **2005**, *6*, 2163.

(5) Product specification for Evidots nanomaterials and Evidtags from Evident Technologies Inc. See <http://www.evidenttech.com/nanomaterials/evidots/quantum-dot-research-materials.php>.

Table 1. DNA Sequences and Their Abbreviations Used in This Study

| DNA code | sequence |
|----------|---|
| DNA-T | H ₂ NC ₆ H ₁₂ -5'-CAT AAA AGA GCT CCA TAT CCA ACC TGC ACG-3' |
| DNA-1 | Alexa 594-3'-GTA TTT TCT CGA GGT ATA GGT TGG ACG TGC-5' |
| DNA-C | 3'-GTA TTT TCT CGA GGT ATA GGT TGG ACG TGC-5' |
| DNA-NC | 3'-AAT CAG GGA TTT ACG TGC ACG ACA CAC ACT-5'-Alexa 594 |



is where most of the overall QD donor size comes from. In this regard, functional thiols are very useful because QDs have high affinity for thiols, and a range of functional hydrophilic groups can be introduced to the QD surface to achieve water solubility. Furthermore, the size of the resulting water-soluble QD can be tailored by controlling the length of the linker between the thiol and functional terminal group.^{6,7} We have recently shown that direct coupling of thiolated fluorophore-labeled double-stranded DNA to the QD reduces the donor–acceptor distance and significantly enhances the FRET efficiency especially at low DNA/QD copy numbers (i.e., 1:1).⁸ However, to date, specific detection of target DNA via QD-sensitized FRET in covalently coupled QD–DNA systems where the QD is capped with functional thiols has not been demonstrated. This is presumably because DNAs can strongly, nonspecifically, and irreversibly adsorb on the QD surface in competition with specific hybridization.^{7,8} The use of labeled DNAs adsorbed on the QD surface mediated by a positively charged polymer and FRET signal reduction in response to specific hybridization have recently been reported.⁹ However, this is a signal-off approach. A signal-on approach that eliminates nonspecific DNA adsorption should be more useful because it can potentially offer higher sensitivity. In this letter, we report our development of such a signal-on approach with a compact, covalently coupled QD–DNA conjugate, where the capturing DNA is coupled to the QD surface via a tri(ethylene glycol) linker to resist DNA nonspecific adsorption. We show this system is suitable for both label and label-free detection of specific DNA at low DNA probe/QD copy numbers with a sensitivity of ~ 1 nM on a conventional fluorimeter.

Experimental Section

Materials. All chemicals, including *N*-(3-dimethylaminopropyl)-*N*-ethylcarbodiimide hydrochloride (EDC, 99%), *N*-hydroxysuccinimide (NHS, 98%), sodium bicarbonate, DNase- and RNase-free NaCl, high-performance liquid chromatography (HPLC) grade ethanol, methanol, and chloroform, were purchased from Sigma-Aldrich (Dorset, U.K.) and used as received unless otherwise stated. Trioctylphosphine oxide-capped CdSe/ZnS core/shell QDs (TOPO-QD, crystal diameter ~ 2.6 nm, 1.3 mg/mL in toluene) were purchased from Evident Technologies (Troy, NY). The QD emission peaks at 553 nm with a quantum yield of $\sim 30\%$. All DNAs employed in this study were purchased from IBA GmbH (Göttingen, Germany) and used as received unless otherwise stated. The DNA sequences and their abbreviations are given in Table 1. The 5'-C₆-amine-modified capture target strand (DNA-T) and unlabeled DNA probe (DNA-C) are of HPLC grade, and the Alexa 594-labeled DNAs were double HPLC purified by the supplier. PBS buffer (10 \times ; 100 mM phosphate,

1.50 M NaCl, 10 mM NaN₃, pH 7.2), phosphate buffer (20 mM phosphate, pH 6.0), and sodium bicarbonate buffer (50 mM NaHCO₃, pH 9.0) were prepared with ultrapure MilliQ water (resistance > 18 M Ω cm). Unless otherwise stated, water means MilliQ water in this paper.

11-Mercaptoundecyl tri(ethylene glycol) alcohol (EG₃OH) was synthesized following a literature method.¹⁰ The crude compound was purified using flash column chromatography on silica (10% ethanol in ethyl acetate) to yield the final product (EG₃OH) as a colorless oil. ¹H NMR (250 MHz, CDCl₃, δ ppm): 1.20–1.37 (m, 14H, 7CH₂), 1.49–1.60 (m, 4H, 2CH₂), 2.46 (q, 2H, *J* = 7.0 Hz, HSCH₂–), 3.05 (s, br, 1H, –OH), 3.40 (t, 2H, *J* = 7.0 Hz, –CH₂–EG), 3.50–3.75 (m, 12H, 3(OCH₂CH₂)). ¹³C NMR (62.5 MHz, CDCl₃, δ ppm): 72.5, 71.4, 70.5, 70.3, 69.9, 61.5, 34.0, 33.7, 30.5, 29.5, 29.4, 29.0, 28.8, 28.7, 28.3, 26.0, 24.5. HRMS (Q-TOF, ES⁺): found, 359.2222; required for C₁₇H₃₆O₄Sn [M + Na]⁺, 359.2232.

11-Mercaptoundecyl tri(ethylene glycol) acetic acid (EG₃COOH) was synthesized following a literature procedure as shown schematically in Scheme 1.¹¹ A modification of the last step was used, where both protection groups, the thioacetate and *t*-butyl carboxylic acid ester, were simultaneously removed in a single step in 0.1 M HCl in a mixed aqueous/methanol solution heated at reflux. This reduced the synthesis by one step and more importantly improved the overall yield of the final product. The crude compound was purified using flash column chromatography on silica (10% ethanol in ethyl acetate) to yield the final product as a colorless oil. ¹H NMR (250 MHz, CDCl₃, δ ppm): 1.10–1.30 (m, 14H, 7CH₂), 1.40–1.52 (m, 4H, 2CH₂), 2.40 (q, *J* = 7.3 Hz, 2H, HSCH₂–), 3.33 (t, *J* = 6.9 Hz, 2H, –CH₂–EG), 3.44–3.64 (m, 12H, 3(EG)), 4.06 (s, 2H, –CH₂COOH). ¹³C NMR (100 MHz, CDCl₃): 170.8 (C=O), 71.4, 70.9, 70.6, 70.0, 68.6, 51.7, 34.0, 29.6, 29.4, 29.0, 28.3, 26.0, 24.6. HRMS (TOF ES[–]): found, 393.2326; required for C₁₉H₃₇O₆S [M – H][–], 393.2312.

EG₃OH/EG₃COOH-capped QDs were prepared by a ligand exchange procedure as outlined below.¹² First, the trioctylphosphine oxide (TOPO)-QD was precipitated by adding ~ 1 mL of the

(6) (a) Pathak, S.; Choi, S.-K.; Arnheim, N.; Thompson, M. E. *J. Am. Chem. Soc.* **2001**, *123*, 4103. (b) Uyeda, H. T.; Medintz, I. L.; Jaiswal, J. K.; Simon, S. M.; Mattoussi, H. *J. Am. Chem. Soc.* **2005**, *127*, 3870. (c) Wang, Q.; Xu, Y.; Zhao, X.; Chang, Y.; Liu, Y.; Jiang, L.; Sharma, J.; Seo, D.-K.; Yan, H. *J. Am. Chem. Soc.* **2007**, *129*, 6380. (d) Susumu, K.; Uyeda, H. T.; Medintz, I. L.; Thomas, P.; Delehanty, J. B.; Mattoussi, H. *J. Am. Chem. Soc.* **2007**, *129*, 13987. (e) Wang, Q.; Liu, Y.; Ke, Y.; Yan, H. *Angew. Chem., Int. Ed.* **2008**, *47*, 316.

(7) Zhou, D. J.; Piper, J. P.; Abell, C.; Klenerman, D.; Kang, D. J.; Ying, L. M. *Chem. Commun.* **2005**, 4807.

(8) Algar, W. R.; Krull, U. J. *Langmuir* **2006**, *22*, 11346.

(9) Peng, H.; Zhang, L.; Kjallman, T. H. M.; Soeller, C.; Travas-Sejdic, J. J. *Am. Chem. Soc.* **2007**, *129*, 3048.

(10) (a) Prime, K. L.; Whitesides, G. M. *J. Am. Chem. Soc.* **1993**, *115*, 10714. (b) Zhou, D.; Bruckbauer, A.; Ying, L. M.; Abell, C.; Klenerman, D. *Nano Lett.* **2003**, *3*, 1510. (c) Zhou, D. J.; Wang, X. Z.; Birch, L.; Rayment, T.; Abell, C. *Langmuir* **2003**, *19*, 10557.

(11) Roberts, C.; Chen, C. S.; Mrksich, M.; Martichonok, V.; Ingber, D. E.; Whitesides, G. M. *J. Am. Chem. Soc.* **1998**, *120*, 6548.

stock toluene solution to ~10 mL of ethanol, and the resulting suspension was centrifuged at 14 000 rpm for 5 min. The clear supernatant was discarded. The pellet was dissolved in ~0.5 mL of toluene and precipitated by ethanol, followed by centrifugation. The clear supernatant was discarded. This process was repeated twice to remove uncapped free TOPO ligands that could interfere with the ligand exchange reaction. The pellet was finally dissolved in 1 mL of CHCl_3 and transferred to a 50 mL round-bottom flask, into which 3 mL of ethanol solution of a 2:1 mixture of the $\text{EG}_3\text{OH}/\text{EG}_3\text{COOH}$ (total thiol concentration 50 mM) and tetramethylammonium hydroxide (1.3 mol equiv to the total amount of thiols) in methanol was added. The resulting solution was heated at reflux for 4 h under a N_2 atmosphere. After the solution was cooled to room temperature, the solvent was removed under reduced pressure. The residue was dissolved in ~0.5 mL of ethanol, and CHCl_3 (~5 mL) was added to precipitate the $\text{EG}_3\text{OH}/\text{EG}_3\text{COOH}$ -capped QDs. The resulting suspension was centrifuged at 14 000 rpm for 10 min, and the clear supernatant was discarded. The pellet was then dissolved in ethanol and precipitated by CHCl_3 , followed by centrifugation, discarding the clear supernatant. The process was repeated three times to remove any uncapped free thiols. Finally, the pellet was dissolved in ~2 mL of EtOH/water (1:1, v/v) to obtain the stock solution. The concentration of the QDs was calculated using the absorbance at the first exciton peak and the extinction coefficient of $98\,000\text{ M}^{-1}\text{ cm}^{-1}$ provided by the manufacturer.

Preparation of the QD–DNA–T Conjugate. EDC (30 mg) and NHS (15 mg) were dissolved in 200 μL of 1:1 (v/v) EtOH/ H_2O mixture, into which 200 μL of phosphate buffer (20 mM, pH 6.0) was added and thoroughly mixed. After that, 250 μL of the $\text{EG}_3\text{-OH}/\text{EG}_3\text{COOH}$ -capped QDs (4 μM in water) was added and thoroughly mixed, and the solution was sonicated in an ultrasonication bath for 20 s and then allowed to stand at room temperature for 1 h. The solution was then centrifuged at 14 000 rpm for 10 min, and the clear supernatant (checked by a UV lamp) was discarded. The red pellet was carefully washed with water ($2 \times 200\ \mu\text{L}$) to remove any residual unreacted EDC/NHS. The pellet was then added to 175 μL of MeOH/ H_2O (1:1), followed by 25 μL of C_6 -amine-modified DNA–T (440 μM , the ratio of DNA–T/QD = 11:1) and 100 μL of NaHCO_3 buffer (50 mM, pH 9.0). The mixture was sonicated for 2 min to break up the pellet, and then the solution was stored at 4 °C overnight to obtain a slightly brownish solution. The sample was centrifuged at 14 000 rpm for 20 min, and the clear supernatant was carefully separated from the pellet. The pellet was washed with 200 μL of MeOH/ H_2O (1:1). A UV–vis absorption spectrum was taken on the combined supernatant, and the absorbance at 260 nm was used for the calculation of the amount of DNAs not conjugated to the QD using a molecular extinction coefficient of $292\,000\text{ M}^{-1}\text{ cm}^{-1}$ for DNA–T, as provided by the manufacturer (the supernatant was first checked with a UV lamp to ensure it was free of QDs, otherwise the strong absorption of the QDs at 260 nm will interfere with the measurement). The number of DNA–T attached to each QD was estimated to be 2.2, and thus, a coupling efficiency of 20% was obtained based on a starting DNA–T/QD ratio of 11. The pellet was added to 0.5 mL of pure water, sonicated for 5 min to obtain a clear stock solution, and stored in the dark at 4 °C until use.

Hybridization of Probe DNAs with the QD–DNA–T Conjugate. The total volume of the hybridization reaction solution was kept constant at 500 μL , with a final QD concentration of 100 nM in $1 \times \text{PBS}$. The reaction was carried out in batches under identical conditions, where 50 μL of $10 \times \text{PBS}$, the calculated amount of pure water, (ethidium bromide where necessary), DNA probe (this varies in different DNA probe/QD ratios), and the required amount of the QD–DNA–T conjugate were sequentially added to a series of Eppendorf tubes and thoroughly mixed on a vortex mixer. The hybridization reaction was carried out at room temperature for 2 h before fluorescence spectra were taken. For kinetic studies, the required QD–DNA–T conjugate solution in $1 \times \text{PBS}$ was prepared

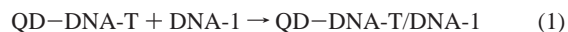
and transferred to a fluorescence cuvette, and a fluorescence spectrum was taken. A calculated amount of DNA–1 was then added and quickly mixed with a micropipet. Fluorescence spectra were then recorded at different reaction intervals to obtain kinetic information. The dilution of the QD–DNA–T conjugate resulting from the increased volume following the addition of DNA–1 was corrected for.

UV–Vis Spectra. The absorption spectra of the QD–DNA conjugates were measured on a Cary 300 Bio UV–vis spectrophotometer (Varian Inc., CA). A spectral range of 220–800 nm was recorded at a scan rate 600 nm/min at a slit width of 2 nm with a quartz cuvette. The spectral background was corrected with blank $1 \times \text{PBS}$ buffer using the same cuvette.

Fluorescence Spectra. All fluorescence spectra were recorded on an Aminco–Bowman Series 2 Luminescence spectrometer (Sim-Aminco Spectronic Instruments Inc, Rochester, NY).⁵ The emission spectra (500–800 nm range) were recorded under a fixed excitation wavelength of 445 nm (to minimize direct excitation of the Alexa 594 dye) at a scan rate of 2 nm/s. An excitation and emission bandwidth of 4 nm was used. For the QD–DNA conjugates, where the DNA was labeled with the Alexa 594 fluorophore, the fluorescence spectra were corrected for direct excitation of the dye by using the same dye-labeled DNA as reference. The quantum yield of the QD was measured using Rhodamine-6G in ethanol (95% under 480 nm excitation) as a reference. The optical densities of the QD and Rhodamine-6G solutions used were 0.05 at 480 nm. Since the fluorescence quantum yield of QDs in the QD–DNA conjugates is dependent on the number of DNAs attached to each QD, the approximate FRET efficiency was estimated using $E = I_A/(I_A + I_D)$, where I_D and I_A are donor and acceptor fluorescence intensities, respectively, rather than using donor quenching.

Calculation of the FRET Signal. The fluorescence intensity referred to in this paper is the integrated fluorescence. The Alexa 594 fluorescence from the hybridized sample was obtained using the integrated fluorescence of the whole spectrum (after correction for direct excitation of Alexa 594) after subtracting the QD fluorescence. The calculation was carried out assuming that the QD fluorescence maintained the same shape as that of the QD–DNA–T conjugate only sample, so its integrated fluorescence is proportional to the height of the QD fluorescence peak (Alexa 594 does not fluoresce at the QD fluorescence peak, 558 nm).

Fitting of the Hybridization Kinetic Data. Two assumptions have been used to fit the kinetic data: (1) the FRET signal arises from the 1:1 hybridized QD–DNA–1 conjugate and (2) the maximum FRET signal corresponding to a QD–DNA–T/DNA–1 conjugate concentration equals the QD starting concentration. This assumption is needed to estimate the percentage of the QD–DNA–T conjugate hybridized. These assumptions are reasonable because the hybridization reactions were carried out at concentrations much higher than the dissociation constant ($K_d < 1\text{ nM}$) of a 30-mer duplex DNA. The hybridization reaction can be described as



where the starting concentrations for the QD–DNA–T and DNA–1 are the same, $C_{\text{QD}} = C_{\text{DNA–1}} = C_0$.

So, the rate of the hybridization reaction can be described by second-order kinetics as

$$dC/dt = k_A C_{\text{QD}} C_{\text{DNA–1}} = k_A [C_0 - C]^2 \quad (2)$$

where k_A is the hybridization rate constant and C is the concentration of the QD–DNA–T/DNA–1 conjugate. Thus

$$dC/[C_0 - C]^2 = k_A dt \quad (3)$$

At the beginning of the hybridization reaction, when $t = 0$, $C = 0$. Integration of the equation gives

$$C/C_0 = 1 - 1/(C_0 k_A t + 1) = 1 - 1/(kt + 1) \quad (4)$$

(12) (a) Wuister, S. F.; Swart, I.; van Driel, F.; Hickey, S. G.; Donega, C. D. *Nano Lett.* **2003**, *3*, 503. (b) Zhou, D. J.; Bruckbauer, A.; Abell, C.; Klenerman, D.; Kang, D.-J. *Adv. Mater.* **2005**, *17*, 1243.

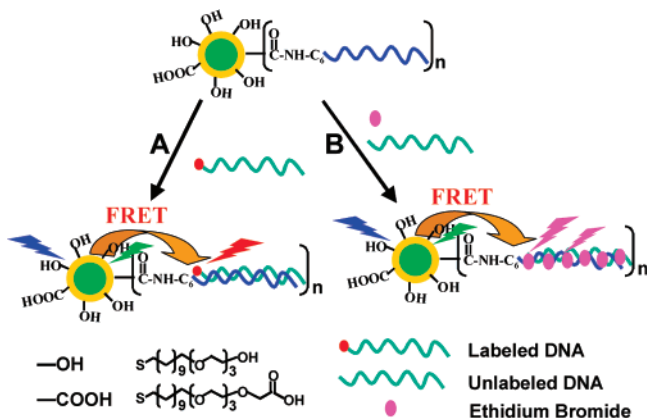


Figure 1. Schematic representation of the principles of our approaches for hybridization and label-free detection of DNA probes with a covalently coupled QD–DNA–T conjugate via a QD sensitized FRET signal.

where $k = C_0 k_A$. Since the fluorescence of the QD–DNA–T conjugate can gradually degrade when exposed to PBS, a factor for this correction is also added (assuming the degradation is linear with incubation time). Thus, the equation used to fit the curve is

$$C/C_0 = 1 - 1/(kt + 1) - at \quad (5)$$

All the kinetic curves were fitted using this equation. The value of k_A was obtained from the fitting parameter of k divided by C_0 , the starting concentration.

Results and Discussion

Figure 1 shows our approach schematically. The commercial trioctylphosphineoxide (TOPO)-capped CdSe/ZnS core/shell QDs (emission peak ~ 553 nm, quantum yield $\sim 30\%$) are made water-soluble by ligand exchange with a 2:1 mixture of EG₃-OH/EG₃-COOH in mixed solvents of chloroform/ethanol. This produces stable, water-soluble EG₃-OH/EG₃-COOH-capped QDs, where the functional hydrophilic hydroxyl (OH) and carboxylic acid (COOH) terminal groups are spaced out from the QD surface with a tri(ethylene glycol) (EG₃) spacer. The introduction of the EG₃ group to the surface capping enhances the stability and solubility of the QD in aqueous media^{6d} and more importantly provides a surface coating that resists the nonspecific adsorption of DNAs.¹¹ The functional QD–DNA conjugate was prepared by first activation of the EG₃-OH/EG₃-COOH-capped QD with EDC/NHS in phosphate buffer (pH 6.0), followed by coupling of the 5'-C₆-amine-modified 30-mer target DNA (DNA-T) to the QD surface carboxylate group via the formation of an amide linker in sodium bicarbonate buffer (pH 9.0). Hybridization of a fluorophore (Alexa 594)-labeled DNA complementary to DNA-T brings the fluorophore in close proximity to the QD, so when the QD is excited, it efficiently undergoes energy transfer to the fluorophore via FRET, producing a dye fluorescence signal that can be used for detection of the labeled complementary DNA probe (route A). Noncomplementary probes do not hybridize to the QD–DNA–T conjugate, so they do not participate in the FRET process and are therefore nonfluorescent. This makes the removal of such probes unnecessary, a distinct advantage for the FRET-based system. Alternatively, an unlabeled complementary DNA and ethidium bromide (EB), a dye known to specifically intercalate double-stranded DNAs,¹⁴ are simultaneously intro-

duced to the system. The formation of duplex DNA via hybridization leads to EB intercalation,¹⁴ so excitation of the QD leads to energy transfer from the QD to EB, producing EB fluorescence that can be used for detection and quantification of unlabeled DNAs (route B). This should be more useful from the sensor application point of view, because it does not require labeling of the probes. Noncomplementary probes will not produce any EB FRET signal because they cannot hybridize to the QD–DNA–T conjugate, and so no EB will intercalate.

To make a highly water-soluble EG₃-OH/EG₃-COOH-capped QD, it is important to remove the free TOPOs in the QD stock solution, otherwise incomplete ligand exchange will produce a QD of poor aqueous solubility. The water-soluble EG₃-OH/EG₃-COOH-capped QD prepared in this study was stable for at least 1 month when stored in the dark at 4 °C. No changes in the fluorescence intensity and spectral shape were observed within this period. It maintains a sharp emission band (fwhm ~ 30 nm) similar to that of the original TOPO-QD, with a slight red-shift of the emission peak to 558 nm. The quantum yield is $\sim 15\%$, about half that of the original TOPO-QD, but this still compares favorably to most of the commercial water-soluble QDs.⁷ The QD emission significantly overlaps the absorption of the Alexa 594 fluorophore, the acceptor used for DNA labeling, so efficient FRET can be obtained in this system (Supporting Information, Figure S1). Based on the spectral overlap and the molecular extinction coefficient of Alexa 594, a Förster distance R_0 of ~ 4.2 nm is estimated for this QD–Alexa 594 FRET system.⁷ On average, there are 2.2 DNA–T molecules attached to each QD in our QD–DNA–T conjugate prepared in this study.

Hybridization of complementary DNA-1 (labeled with Alexa 594 at 3'; see Table 1) to the QD–DNA–T conjugate was carried out using 100 nM QD in 1 \times PBS (10 mM phosphate, 150 mM NaCl, pH 7.2) at different DNA-1/QD ratios. The corresponding fluorescence spectra (all corrected for background from direct dye excitation) are shown in Figure 2A. It is clear that hybridization of DNA-1 to the QD–DNA–T conjugate quenches the QD emission at 558 nm while enhancing the emission of Alexa 594 at 618 nm via FRET. The apparent FRET efficiency, $E = I_A/(I_A + I_D)$, where I_A and I_D are the integrated acceptor (Alexa 594) and donor (QD) fluorescence (see Experimental Section for details),^{2,3,7} increases approximately linearly with the increasing copy numbers of DNA-1 per QD initially, and then it levels off at a ratio of just over 2 (Figure 2B). This is in excellent agreement with the estimation that there are only 2.2 DNA–Ts attached to each QD. This confirms that all the DNA–T molecules coupled to the QD are functional and available for hybridization. We found that the use of PBS is crucial to achieving specific hybridization. Another buffer, such as Tris (10 mM Tris HCl, 100 mM NaCl, pH 7.6), produced significant nonspecific DNA adsorption.

To confirm that the observed FRET signal is due to specific DNA hybridization, and not from nonspecific adsorption, three control experiments were carried out. (1) The EG₃-OH/EG₃-COOH-capped QD (100 nM) without any DNA–Ts attached was mixed with DNA-1 (220 nM) in 1 \times PBS under identical conditions. This did not produce any detectable Alexa 594 FRET signal (Supporting Information, Figure S2A). This eliminates the possibility that the FRET signal is due to the nonspecific adsorption of DNA-1 on the QD surface. (2) The QD–DNA–T conjugate (100 nM) and DNA-1 (220 nM) were mixed in pure water without salt. No Alexa 594 FRET signal was detected, suggesting that no hybridization had taken place. However, upon addition of 50 mM NaCl (final concentration) to this system, a significant FRET signal was observed, confirming that DNA

(13) Sekar, M. M. A.; Bloch, W.; Pamela, M.; St John, P. M. *Nucleic Acids Res.* **2005**, *33*, 366.

(14) He, F.; Tang, Y.; Yu, M.; Feng, F.; An, L.; Sun, H.; Wang, S.; Li, Y.; Zhu, D.; Bazan, G. C. *J. Am. Chem. Soc.* **2006**, *128*, 6764.

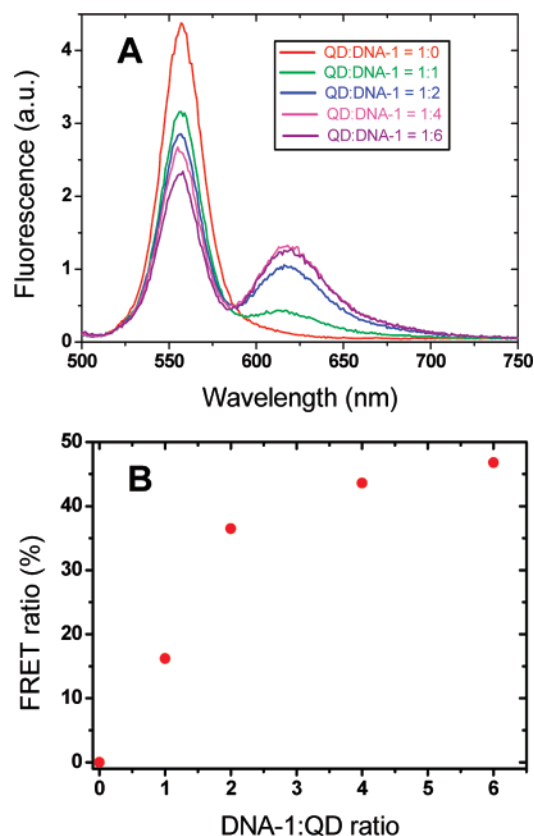


Figure 2. (A) Fluorescence spectra of the QD–DNA–T conjugate after hybridization with DNA-1 at different molar ratios. All experiments were carried out in $1 \times$ PBS with 100 nM QD–DNA–T conjugate excited at 445 nm. (B) Plot of the apparent FRET efficiency versus the DNA-1/QD ratios.

hybridization did take place (Supporting Information, Figure S2B). It is well-known that DNA hybridization is salt dependent; without the salt counterions to shield the strong electrostatic repulsion from the negatively charged phosphate backbones, the DNA duplex could not form. The fact that the Alexa 594 FRET signal is only observed in the presence of moderate salt supports that the FRET signal is indeed due to DNA hybridization. (3) Alexa 594-labeled control DNA (DNA-NC, 30-mer but with a noncomplementary sequence to DNA-T) was incubated with the QD–DNA–T conjugate. This produced no detectable Alexa 594 FRET signal (Supporting Information, Figure S2C). The three control experiments confirm unambiguously that the observed Alexa 594 FRET signal is indeed due to the specific hybridization between complementary DNAs. This is a significant improvement in covalently coupled QD–DNA systems, where other systems lacking the EG₃ spacer have exhibited strong nonspecific adsorption of DNAs,⁸ suggesting that the introduction of the EG₃ linker to the QD surface coating effectively eliminates the nonspecific adsorption of DNA on the QD surface. This suggests that this system is suitable for specific detection of labeled complementary probes.

Figure 3 shows the time-dependent hybridization induced FRET signal between the DNA-1 and QD–DNA–T conjugate at a fixed DNA-1/QD ratio of 1:1 at different concentrations. Compared with other covalent QD–DNA systems, where a complete hybridization requires over 8 h,⁸ our system is ~ 50 times faster and is complete in ~ 10 min. This suggests that the DNA-Ts in our system are not significantly hindered and can readily hybridize. The time-dependent fluorescence can be fitted to second-order reaction kinetics (See Experimental Section for details of the fitting). The value of the hybridization rate constant

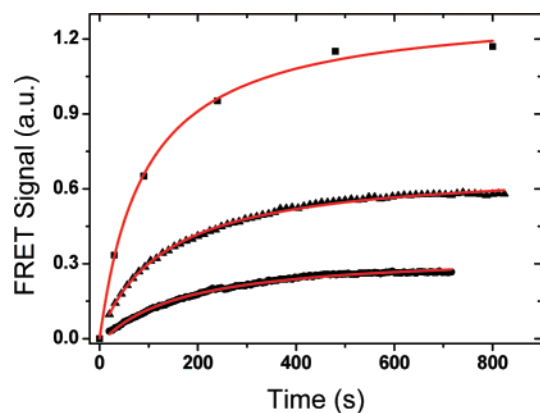


Figure 3. Time-dependent FRET signal showing the hybridization kinetics between QD–DNA–T and DNA-1 at a 1:1 ratio at 100 nM (solid squares), 50 nM (filled triangles), and 25 nM (filled circles). The red lines are the fits using a second-order reaction kinetics as described in the experimental section.

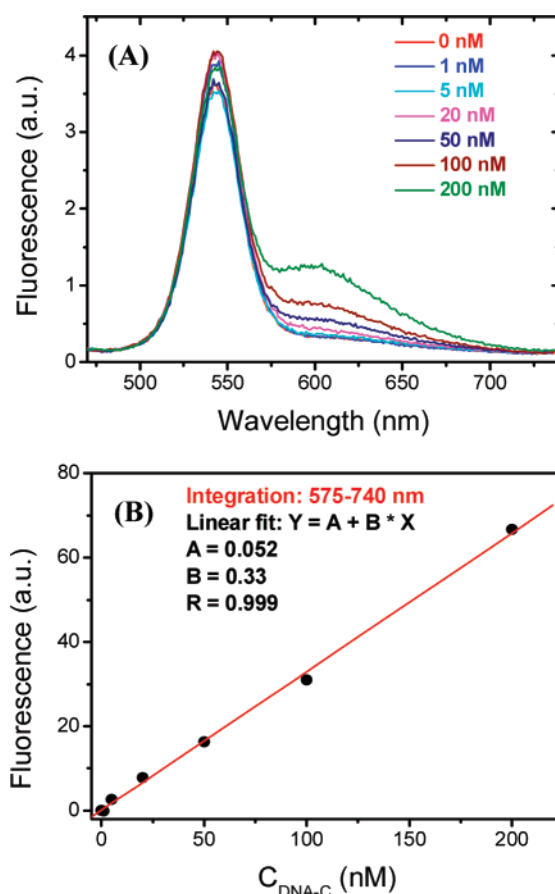


Figure 4. (A) Fluorescence spectra of the QD–DNA–T conjugate for label-free detection of DNA-C. The spectra were recorded in PBS excited at 378 nm. (B) A plot of the EB FRET signal (integrated fluorescence from 575 to 740 nm, background corrected) versus the concentration of DNA-C.

k_A can be obtained from the fitting parameter of k divided by C_0 , the starting concentration. The best fitting parameter k is 0.017 ± 0.002 , 0.0081 ± 0.0003 , and 0.0072 ± 0.0002 s⁻¹ for the 100, 50, and 25 nM samples, respectively. This gives a k_A value of 1.7 ± 0.2 , 1.6 ± 0.1 , and $2.9 \pm 0.1 \times 10^5$ M⁻¹ s⁻¹ for the 100, 50, and 25 nM samples, respectively. These values are comparable to those of free DNAs without a secondary structure,¹³ suggesting that conjugation of DNA-T to the QD surface does not affect the hybridization kinetics significantly.

Having demonstrated that this QD–DNA–T conjugate is functional and can be used for specific detection of labeled complementary probes at low probe/QD copy numbers, a more important step was to investigate its potential for detecting unlabeled probes. In this regard, we have explored a strategy based on the fact that ethidium bromide (EB) specifically intercalates duplex DNA without sequence specificity, as the fluorescence readout (Figure 1, route B).¹⁴ These experiments were carried out under the same experimental conditions as before, where each sample contained 100 nM QD–DNA–T conjugate, 3 μ M EB, and different concentrations of unlabeled complementary DNA–C and was allowed to hybridize for 2 h. The corresponding fluorescence spectra are shown in Figure 4A. It is clear that the EB fluorescence increases with increasing DNA–C concentration. Introduction of a noncomplementary unlabeled DNA (500 nM) to the (QD–DNA–T + EB) system did not produce any observable EB fluorescence, confirming that the observed EB FRET signal is DNA sequence specific. This is presumably because EB binds strongly to double-stranded DNAs without any sequence specificity,¹⁴ whereas, for single-stranded DNAs, EB binding is much weaker and has some sequence specificity.¹⁵ The fact that no EB fluorescence was detected here for the QD–DNA–T/EB system in the absence of DNA–C may suggest that the DNA–T sequence used in this study does not bind EB or the binding is too weak to be detectable under our experimental conditions. A plot of the integrated EB FRET signal versus the concentration of DNA–C shows a very good linear fit ($R = 0.999$, Figure 4B), suggesting that this system is well-suited for label-free detection and quantification of complementary DNA analyte. The detection limit here is ~ 1 nM using

(15) (a) Sarov-Blat, L.; Livneh, Z. *J. Biol. Chem.* **1998**, *273*, 5520. (b) Davies, D. B.; Baranovsky, S. F.; Veselkov, A. N. *J. Chem. Soc., Faraday Trans.* **1997**, *93*, 1559.

a conventional fluorimeter. This can be improved by using shorter alkyl linkers between the QD and DNA–T to improve the FRET efficiency. Even with this by no means optimized system, the sensitivity achieved here is already better than the recently reported QD FRET based on a signal-off approach,⁹ demonstrating the excellent potential of this signal-on approach.

In summary, we have prepared a compact, covalently coupled functional QD–DNA conjugate and demonstrated the detection specific, unlabeled nanomolar complementary DNA via a QD-sensitized Alexa 594 FRET signal at low DNA probe/QD copy numbers. This has been achieved by incorporation of an EG₃ linker into the QD surface coating that effectively eliminated the nonspecific adsorption of DNAs on the QD surface, allowing specific hybridization of complementary DNA to the QD–DNA–T conjugate. Further optimization of this system is currently under way, to reduce the alkyl linker length of the thiol ligand and to improve the stability of the water-soluble QD by using chelating ligands. These developments in combination with the DNA/RNA aptamers¹⁶ will lead to a general, robust, highly sensitive, and selective QD FRET-based sensing platform suitable for the detection of a wide range of targets, from important disease markers and metal ions to drug molecules.

Acknowledgment. This work was supported as part of the University of Cambridge–ETRI (Korean) Joint International Research Collaboration.

Supporting Information Available: Supporting figures showing the absorption and fluorescence spectra of Alexa 594 and their overlapping with QD fluorescence, and fluorescence spectra of the control experiments. This material is available free of charge via the Internet at <http://www.acs.org>.

LA703583U

(16) Bunka, D. H. J.; Stockley, P. G. *Nat. Rev. Microbiol.* **2006**, *4*, 588.